Annealing behaviour of 6061 aluminium deposited by high pressure cold spray

M. R. Rokni*[1], C. A. Widener[1], S. P. Ahrenkiel[2], B. K. Jasthi[1] and V. R. Champagne[3]

Aluminium 6061 deposited by high pressure cold spray was analysed using a transmission electron microscope (TEM) to characterise its microstructure and response to annealing to 450°C in the plane of the deposition and perpendicular to the deposited layers. The cold sprayed deposition was also analysed with scanning electron microscopy (SEM), energy dispersive X-ray spectroscopy (EDS) analysis and differential scanning calorimeter (DSC). Segregation of the solute atoms (Mg and Si) at the grain boundaries during cold spraying was seen to play a crucial role in stabilising the deformation substructure until specific temperatures, and was found to have a significant effect on the annealing behaviour of the microstructure in the two different directions.

Keywords: Aluminium, Cold spraying, Segregation, Annealing, TEM

This paper is part of a special issue on cold spray technology

Introduction

The processing of metals through the application of severe plastic deformation provides the potential for achieving exceptional grain refinement in bulk solids.[1] In general, processing by cold gas dynamic spraying or cold spraying (CS), where solid particles on the order of 50 μm reach velocities ranging normally from 500 to 1000 m s^{-1}, leads to strains up to about 10 (at strain rates of 10^6–5×10^9 s^{-1}). CS also fabricates dense depositions with ultrafine grains (UFG) and even some nanograins (10–100 nm). Additionally, cold spray has been shown to be a potential method for the preparation of commercial scale material quantities and to have the ability to join widely dissimilar materials.[2–9] A number of works have been devoted to commercial aluminium alloys including 1100, 2618 and 5083 through CS processing.[10–12] Most of the previous studies have been conducted in order to understand the deformation mechanisms, the significant parameters of CS processing, and its resulting properties. But less attention has been paid to evaluate the relationship between the microstructures of the particles before deposition and in the resulting cold spray processed (CSP) layer, or the effects of subsequent heat treatment.

In UFG materials, the fraction of grain boundaries (GBs) is much larger than in conventional coarse grained alloys. Often these materials are produced by severe plastic deformation processes. Since these processes include high strain rate conditions and fast cooling rates, some have observed the presence of non-equilibrium grain boundaries (non-equilibrium GBs) in nanostructured materials.[13] Valiev *et al.*[14] defined them as GBs that hold extrinsic dislocations that are not needed to accommodate the misorientation across the GBs. Therefore, non-equilibrium GBs can be ideal candidates for causing segregation in order to reduce their local energy states.[15–18] There is also some indirect evidence of grain boundary segregation in UFG materials processed by cold work,[18–22] which could also be explained by this mechanism. GB segregation is an extremely important phenomenon because it may affect significantly the material properties like corrosion resistance, mechanical behaviour or thermal stability.[15–17] It is thus of great importance to investigate the mechanism of the deformation induced solute redistribution and concurrent GB migration that was observed in the as sprayed deposition of this investigation.

Subsequent to CSP at ambient temperatures, most severely deformed alloys show low tensile ductility. As a result, they must be annealed to obtain the best possible combination of strength and ductility.[23,24] During non-isothermal heat treatment, recovery and precipitation are likely to occur, generating complex interactions with recrystallisation. In addition, the precipitation of dispersoids in the course of an annealing treatment can hinder or even suppress recrystallisation or grain growth.[24] Segregation of solute elements may also play a crucial role in the occurrence of the aforementioned phenomena, which can prevent GB and non-equilibrium GB migration. This can help to retain nanosized grains in the corresponding microstructure.[25–27] Since GBs and non-equilibrium GBs are the main sites for solute segregation, the annealing behaviour of the 6061 CS deposited layer could deviate from the published results of other high strain rate processes.

[1]Department of Materials & Metallurgical Engineering, Advanced Materials Processing Center, South Dakota School of Mines & Technology (SDSM&T), Rapid City, SD, USA
[2]Department of Nanoscience and Nanoengineering, South Dakota School of Mines & Technology (SDSM&T), Rapid City, SD, USA
[3]US Army Research Laboratory, Weapons and Materials Research Directorate, Aberdeen Proving Ground, Aberdeen, MD, USA

*Corresponding author, email mohammadreza.rokni@mines.sdsmt.edu

Published by Maney on behalf of the Institute
Received 24 June 2013; accepted 18 September 2013
DOI 10.1179/1743294413Y.0000000209

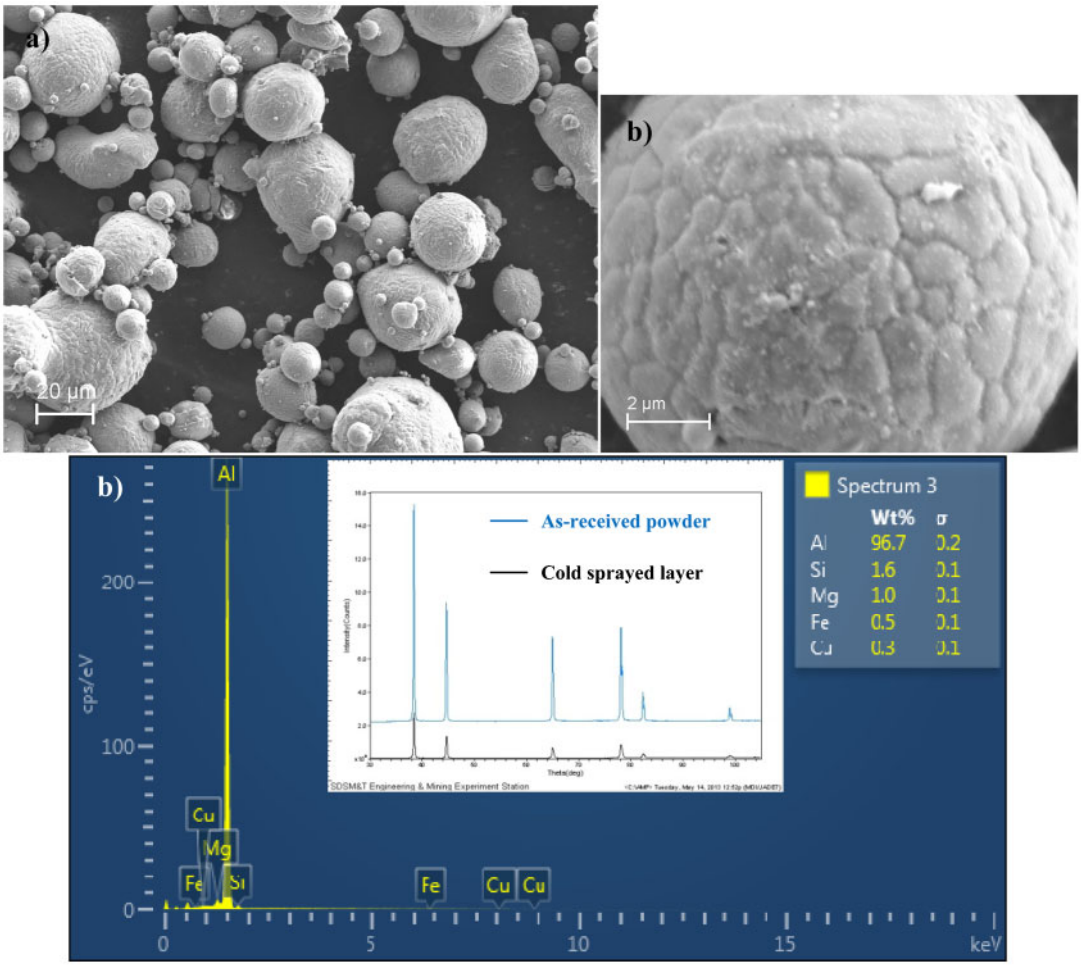

1 ***a*** **SEM image showing powders morphology,** ***b*** **SEM image showing grain structure on powder particles surface and** ***c*** **EDS analysis of as atomised 6061 powder, and inserted XRD pattern for powder and as sprayed deposition**

The present study was undertaken in an effort to understand the recovery and recrystallisation processes and associated changes of microstructures during annealing of an optimised, fully consolidated, high pressure CSP 6061 alloy deposition layer. Characterising the as deposited microstructures and the corresponding changes observed after annealing is important for microstructure control. Toward this end, a hot stage transmission electron microscope (TEM) investigation was found to be a suitable and powerful tool to study and probe the complex interactions during non-isothermal heating and annealing.

Experimental methods

In the present study, a 6061 depositions was produced by a commercial gas atomised 6061 Al powder with size range of 5–50 μm and average size of 38·7 μm (measured with Microtrac S3000 instrument) was used as the feed stock. Helium was used as the process gas to achieve high impact between incident particles. The deposits were made using a CGT 4000 cold spray system and the pressure and temperature of helium were maintained at 28 bar and 400°C respectively.

The powder morphology and the deposition microstructure were examined using a Zeiss Supra 40VP scanning electron microscopy (SEM). Before SEM observation, the deposition samples were sectioned from perpendicular and parallel directions (Y and Z) and prepared by standard metallographic techniques. TEM analysis for the as received powder involved suspending Al powders in acetone, ultrasonicating for 10 min, dipping a copper grid into the solution, drying for 10 min and inserting in a vacuum chamber for an hour before inserting the sample in the TEM chamber. X-ray diffraction (XRD) measurements on the as received powder and the deposited layer precipitates were also carried out. The microstructure of the depositions was also analysed by TEM and high resolution transmission electron microscopy (HRTEM) using a JEM-2100 LaB_6 equipped with a hot stage and energy dispersive X-ray spectroscopy (EDS) analysis, using discs of 3 mm diameter punched from different directions of the deposition, and then polished, dimpled and ion milled for 4 h.

The annealing behaviour of the cold spray deposited material was characterised by heating of the sample to 450°C with 10°C min^{-1} heating rate followed by microstructural characterisation in the Z and Y directions. Thermal analysis was also performed in a SDT Q600 differential scanning calorimeter (DSC) in order to investigate the phase evolution of 6061 deposited sample during the continuous heating. Polished alloy discs with a diameter of 3 mm were sealed in Al pans and heated in a flowing Ar atmosphere at the same heating rate used in the TEM. Two DSC runs were successively performed on each sample with the curve from the second run used as the baseline.

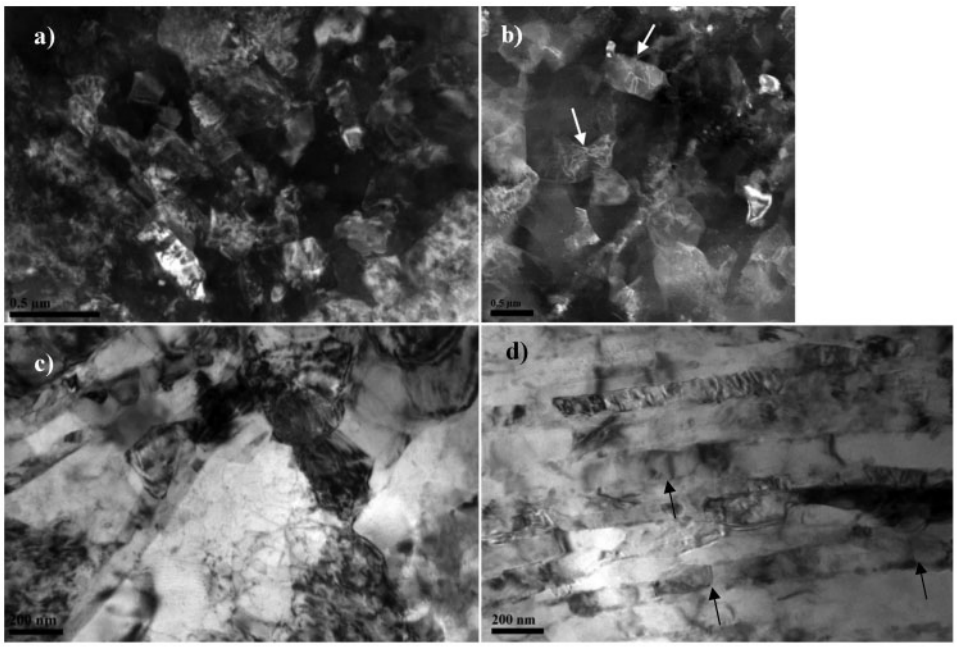

2 TEM images from 6061 deposited layer showing *a* individuals grains size range and high dislocation density inside of heavily strained grains in *Z* direction, *b* scanning TEM image showing presence of nanosubgrains and dislocation structures inside of different grains (white arrows) in *Z* direction, *c* nanorecrystallisation in *Z* direction and *d* elongated nanograins in *Y* direction with transverse low angle grain boundaries (black arrows)

Results and discussion

As received 6061 Al powder

Figure 1*a* shows the microstructure of the feedstock powder in which the spherical shape and size range of the particles can be seen. It also clearly depicts a typical crystallite size in the range of $\sim$40 μm for the as received 6061 Al powder particles. Figure 1*b* suggests that starting powder particles have some stored residual stress inside these powders. Additionally, their microstructure consists of a grain structure with medium and uniform dislocation density and subgrains or substructure inside, which is well supported by the literature.[4,5,28] The EDS analysis of the as atomised 6061 powder is also shown in Fig. 1*c*. The as atomised Al–Mg–Si sample is a supersaturated face centred cubic (fcc) solid solution. In the inserted XRD pattern, only fcc Al reflection peaks, with a distinct shift from the pure fcc Al peaks towards lower diffraction angles, were observed. The lattice parameter of the solid solution is $\sim$0·4088 nm, significantly larger than that of pure Al (0·4050 nm), which can be attributed to the dissolved Mg and Si atoms. But according to the inserted XRD pattern, there is no lattice parameter difference between the as received powder and the as sprayed deposited material, since there is no peak position variation before or after CS. According to the EDS analysis, the Mg and Si contents were found to be $\sim$1·0 and 1·6 at-%, respectively, indicating that all of the Mg and Si atoms were essentially dissolved to form a supersaturated solid solution.

Microstructural evolution of deposited layer

Grain structure and morphology

Figure 2 shows TEM and scanning TEM images from the as deposited 6061 layer in different directions. Individual grains in Fig. 2*a* were produced with sizes ranging from less than 100 nm to a few hundred nanometres, separated by high angle GBs. Some grains are heavily strained and contain a high density of dislocations. Some of these dislocations inside the as deposited layer can be attributed to the presence of dislocations in the as received powder particles. It has also been well established that these dislocations can act as diffusion paths for solute atoms, and provide nucleation sites for precipitation during processing and post-heat treatment respectively, which will be discussed later in this paper. As indicated in Fig. 2*b* by arrows, some of the grains have $\sim$50 nm subgrains or dislocation structures inside, which mean that they have undergone different levels of recovery during the CS. Moreover, since the as received powder has dislocation structures or substructures inside, some of these subgrains can be the consequence of powder particles interacting with one another during the deformation process.

Details in microstructural features

Figure 2*c* and *d* shows TEM images from the cold sprayed deposition microstructure in *Z* and *Y* directions respectively. The high velocity impact of the powders causes high plastic deformation and results in high dislocation density, with recovery and recrystallisation occurring in the deposition during cold spraying in various regions. As it can be seen in Fig. 2*c*, the deformation is clearly inhomogeneous in the *Z* direction, as shown by the mixture of equiaxed and pancaked grains, dislocation cell structure, subgrain, dislocation tangle zone and microbands. Good particle/particle bonds in the as deposited microstructure can be attributed to a higher degree of deformation, which is further related to adiabatic shear instabilities occurring at the particle/particle interface during cold spraying.

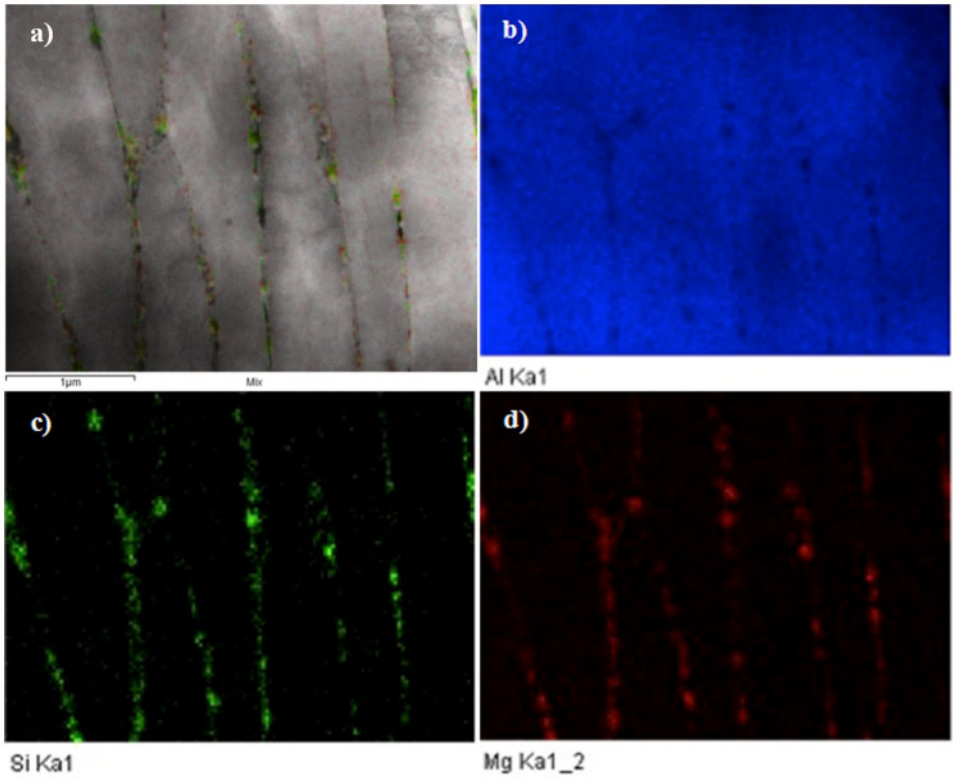

3 *a–d* EDS maps from 6061 deposited layer showing Mg and Si segregation at GBs

The TEM micrograph of the CSP layer in the *Y* direction is seen in Fig. 2*d*, showing lamellar microbands with elongated nanograins inside and well defined GBs. Kikuchi analysis revealed that nearly all of the lamellar boundaries were high angle in character and they thus delineate long thin ribbon shaped grains. Some grains can be seen to extend almost across the entire figure and contain transverse low angle grain boundaries (arrows) with a spacing of 50–200 nm, producing a 'ladder-like', or 'bamboo', structure, which is a common microstructural feature in cold worked materials.[11,21]

Microsegregation of solute elements

Figure 3 shows EDX maps from the CSP 6061 deposited layer in *Y* direction illustrating the occurrence of solutes segregation of Si, Cu and Mg at GBs during the cold spray processing. The presence of these elements at the GBs can result in various precipitates during heating the sample to high temperatures. Accordingly, DSC results presented in Fig. 4 show that there are exothermic peaks in different temperatures providing evidence for precipitation around these temperatures in the substrate and CSP layer, which will be discussed in details later in this paper.

Since the deformation was performed at relatively low temperature (<200°C), no significant increase in the temperature is expected during the CS processing, except the heating resulting from local plastic strain energy release. In such conditions, the mobility of solute elements (Mg and Si) is very low in aluminium and obviously, from the Fick's law [$J=-D\text{grad}(C)$], such a low diffusivity (D) combined with the low solubility (C) of Mg and Si in the aluminium matrix[29] cannot give rise to a significant Mg or Si flux (J) through bulk diffusion. This is also less likely to happen considering the relatively short amount of time (<10 min) for the CSP application at these lower temperatures. Thus, the Mg and Si diffusion observed here might be better explained through other diffusion processes, like pipe diffusion in dislocation cores and vacancies and/or drag mechanisms. It is indeed well known that bulk diffusion rates of solute elements is much lower than their diffusion rates along dislocation cores and vacancies where the activation energy could be lowered by a factor of 2.[20]

During cold spraying, a great number of dislocations and vacancies are developed so that the cold spray introduced defect concentration is very high compared with thermal equilibrium.[3,4,11] Therefore, these excess point defects form defect clusters and/or migrate to defect sink sites such as GBs. Thus, there is a flow of CS introduced point defects towards boundary sinks during CS. As solute atoms prefer grain boundary sites, an increase in global composition would provide more solute atoms to pin GBs and prevent grain growth. This trend has interesting practical benefits because it allows recrystallised nanograins to be explicitly tailored during this deposition process.[30]

The atomic scale mechanism of the CS induced segregation observed in the present study is very similar to that of non-equilibrium segregation resulting from irradiation.[15,31] It is well documented that the oversized elements in alloys preferentially interact with vacancies and diffuse through these point defects, while the undersized elements migrate by both vacancies and dislocation core diffusion mechanisms in the same direction as interstitial atoms.[21,32–35] As a result, it is expected that Mg atoms (oversized element) in solid

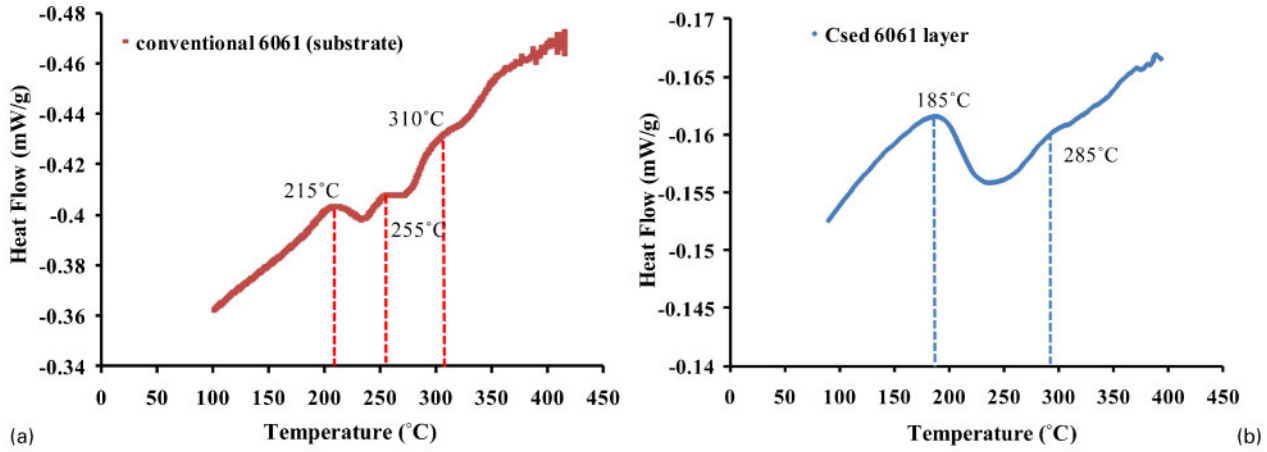

4 DSC curve of 6061 alloy for *a* substrate and *b* CSP layer (scanning rate was set at 10 °C min^{-1})

solution in fcc Al matrix are strongly coupled to vacancies, and the flux of these point defects towards GBs takes place during CS and drags along Mg atoms, which can lead to strong local enrichments at the GBs. Furthermore, Mg atoms being larger than Al, some elastic strain could be relaxed by Mg clusters giving rise to local compressive stresses. Thus, it is reasonable to suppose that Mg segregation may stabilise GBs by reducing their energy.[16,17]

The Si atoms mobility could be enhanced by dislocations since it is an undersized element. A pipe diffusion mechanism along dislocation cores[36] is likely the primary mechanism we observed in operation here, but of course conventional solute drag by dislocations would also be involved in the Si solute segregation.[37] Indeed, due to the enhanced atomic mobility of Si promoted by cold spray induced vacancies, these dislocations could drag a significant amount of Si even at relatively low temperature of cold spray processing and drop them at grain boundaries. One cannot exclude that this mechanism can also work for Mg atoms but not as well as the vacancy diffusion mechanism.[35]

The interplay of stacking fault and solute elements is another effect which can result in the observed solutes segregation. As dislocations dissociate into partial dislocations during CS, the fault energy region is a suitable place for solute elements to be collected. This is due to the elastic strain field of the partial dislocations,[38] which has also been schematically shown in Ref. 35. Thereby, as Varschavsky has reported,[39] solute elements can be transferred to grain boundaries during the processing via diffusion along the pipes of the partials.

Microstructure evaluation after heat treatment under TEM

The TEM images of Z and Y directions of the 6061 deposited layer after annealing to 450°C with 10°C min^{-1} heating rate are shown in Fig. 5. The annealing process involves the loss of some of the stored energy, which provides the driving force for recovery and recrystallisation and the corresponding changes in the microstructure.

The microstructure of the planar view in the Z direction, annealed to 450°C (Fig. 5*a*), shows that the grains in CSP layer are equiaxed with well defined straight grain boundaries instead of elongated grains. The banded contrast observed in this image also indicates that the boundaries are in equilibrium. The generation of the GBs indicates that the compressive stresses are relieved with the formation of interfaces and grains in the microstructure.

Although recrystallisation removes the dislocations, the material still contains grain boundaries, which are thermodynamically unstable. Further annealing may result in grain growth, in which the smaller grains are eliminated, the larger grains grow and the GBs assume a lower energy configuration. As seen in Fig. 5*a*, not only is there a significant reduction in dislocation density after the heat treatment, but also grain growth has occurred in this direction in certain areas.

Figure 5*b* shows that the dislocation loops (arrows) are present in CSP 6061 Aluminium depositions after heat treatment, which can be explained as follows. As mentioned previously in the section on 'As received 6061 Al powder', the feed stock powder has a high dislocation density and cold spraying introduces even more dislocations into the deposition, and they glide, climb and intersect during the processing. As a result, the formation of these loops has to go back to the annihilation of the straight dislocations. This is a process that seems to be related to some special combination of strain, strain rate and temperature rise in the material. These quantities are not known for the given region in the deposition and they are in particular highly non-uniform over the whole CSP layer; so any conjecture on this special combination would be quite speculative. But according to previous published results,[3,40] dislocation loops are stable if their radius R is bigger than about 4a, where a is the lattice constant, which was measured as 0·4088 nm in the present study. Dislocation loops are persistent even after heat treatment,[41] if their diameter exceeds a critical value. The dislocation loops shown in Fig. 5*b*, are on the order of 100–200 nm, which would explain their stability up to annealing temperatures.

Puigví and co-workers[40] studied the interaction between point defects and point defect clusters (loops) in copper by computer modelling. They found that for vacancies self-interstitial recombination is inhibited, and hence, the loops are stable. In addition, Hudson *et al.*[42] have found that single point defects can prevent cluster mobility, which can help the stability of the dislocation loops. With all the above reasoning, it seems rational to

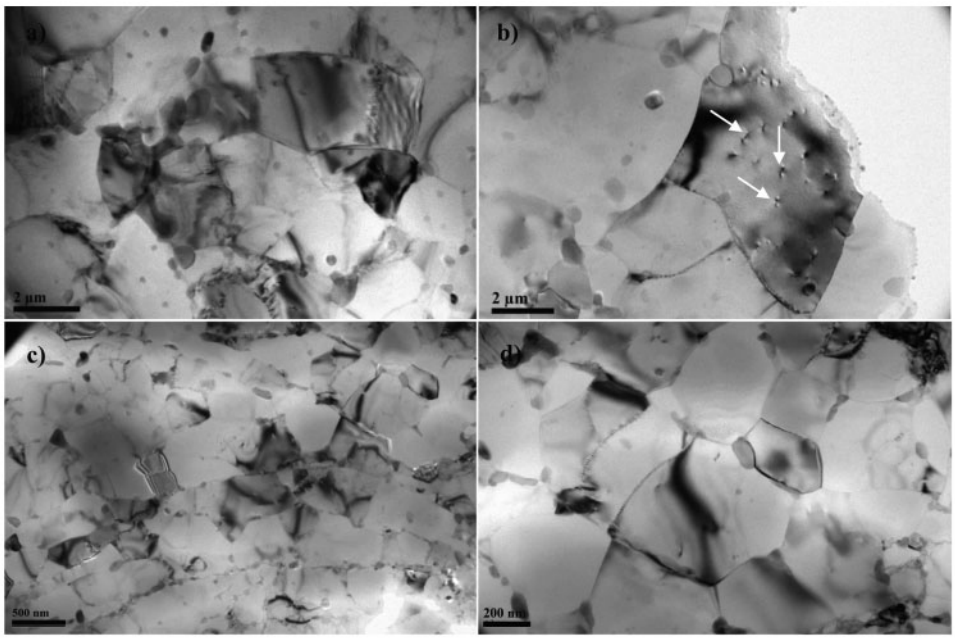

5 TEM images from cold spray deposition after heat treatment to 450°C in different directions: *a Z* direction, occurrence of precipitation and recrystallisation in microstructure; *b Z* direction, low dislocation density inside grains and occurrence of partial grain growth and formation of dislocation loops (white arrows); *c Y* direction, showing presence of some pancaked structure; *d Y* direction, fully recrystallised area without mechanical deformation interfaces between particles

observe dislocation loops in the 6061 CSP layer after the non-isothermal heat treatment. One should note that in aged dilute Al–Mg alloys, it has been already well documented that Mg atoms easily segregate along dislocation loops.[29] Similar features have been reported in irradiated materials where the typical loop size resulting from the agglomeration of point defects was in the range of 10–20 nm.[33]

Figure 5*c* shows the TEM images from the *Y* direction of the 6061 CSP deposited layer after the heat treatment. While its microstructure after CS and before annealing contained a high fraction of non-equilibrium GBs and a high inherent dislocation density, the thermal activation during annealing facilitated restoration processes. As seen in Fig. 5*c* and *d*, the average grain size in this direction is much lower than the perpendicular direction, which has been attributed to a high level of GB solute segregation in this direction. Aust and Rutter[43] and Wang *et al.*[27] have shown that the rate of GB migration could be reduced dramatically even by small average solute concentrations. The latter also proved that the drag force increases with increasing boundary velocity at small velocities and it decreases with increasing velocity at large velocities. In the present research, the heating rate is low enough not to make a high driving force for grain boundaries to migrate, and consequently, the GBs velocities are small and causing a higher drag force to be applied on the GBs.

In addition, the DSC curve for the substrate (Fig. 4*a*), as mentioned before, shows several exothermic peaks at 215, 255 and 310°C demonstrating the occurrence of precipitation around these temperatures. Dunlop *et al.*[44] have reported the corresponding precipitates for these temperatures are MgSi, β'' and β'/B', respectively. As seen in Fig. 4*b*, the DSC curve has shifted to lower temperatures and the β'' peak appears to be missing. The former can be explained by the presence of a high degree of cold work due to very high strain rates in the cold spray process. Determining the reason for the missing peak would require some additional investigation; however, it may be that the first two DSC peaks for the substrate have overlapped in the CSP layer, or that the β'' precipitates are already present in the microstructure. These precipitation processes can occur rapidly due to the very high local supersaturation of precipitate forming elements at the GBs (Fig. 3). Furthermore, during a heat treatment cycle, precipitates that nucleate and grow at the GBs can also have a strong pinning effect on the GBs and prevent grain growth.

Conclusion

This study was undertaken to explore the annealing behaviour of an optimised, fully consolidated, high pressure CSP 6061 aluminium alloy depositions. The microstructural evolution in the deposition after cold spraying and subsequent annealing to 450°C was investigated via different electron microscopes (TEM, HRTEM, EBSD and SEM). The main conclusions from this work are as follows:

1. Cold spraying has been successfully used to obtain highly dense nanocrystalline 6061 aluminium alloy depositionss demonstrating CS as a promising new technique for producing bulk nanostructured metal materials.

2. Feedstock powders with a spherical shape and in the size range of $\sim$40 μm possess medium and uniform dislocation density. The powder structure consisted mainly of subgrains or substructure.

3. The formation of solute segregation in the CSP 6061 layer is attributed to the generation of 'non-equilibrium' GBs. It is also thought that Mg and Si, as oversized and undersized elements, are strongly coupled

to vacancies and dislocations respectively, which leads to strong local solute enrichments.

4. The microstructure of the planar view (Z direction) annealed to 450°C shows that the grains in the CSP layer are equiaxed with well defined straight grain boundaries instead of elongated grains in the CSP deposition.

5. CSP 6061 aluminium depositions were found to be resistant to grain growth in Y direction even upon heat treatment at 450°C owing to the presence of solutes segregation and precipitates at the GBs causing a strong pinning effect on the moving grain boundaries and lower their rate of migration during recrystallisation and/or grain growth.

Acknowledgements

This work was performed under subcontract to the Pueblo Economic Development Corporation under Army Research Lab contract no. W911NF-11-2-0014.

References

1. W. B. Choi, L. Li, V. Luzin, R. Neiser, T. Gnaupel-Herold, H. J. Prask, S. Sampath and A. Gouldstone: 'Integrated characterization of cold sprayed aluminum depositionss', *Acta Mater.*, 2007, **55**, 857–866.
2. P. D. Eason, J. A. Fewkes, S. C. Kennett, T. J. Eden, K. Tello, M. J. Kaufman and M. Tiryakioğlu: 'On the characterization of bulk copper produced by cold gas dynamic spray processing in as fabricated and annealed conditions', *Mater. Sci. Eng. A*, 2011, **A528**, 8174–8178.
3. S. R. Bakshi, D. Wang, T. Price, D. Zhang, A. K. Keshri, Y. Chen, D. G. McCartney, P. H. Shipway and A. Agarwal: 'Microstructure and wear properties of aluminum/aluminum–silicon composite depositionss prepared by cold spraying', *Surf. Coat. Technol.*, 2009, **204**, 503–510.
4. Y. Zou, W. Qin, E. Irissou, J. G. Legoux, S. Yue and J. A. Szpunar: 'Dynamic recrystallization in the particle/particle interfacial region of cold-sprayed nickel depositions: electron backscatter diffraction characterization', *Scr. Mater.*, 2009, **61**, 899–902.
5. Y. Zou, D. Goldbaum, J. A. Szpunar and S. Yue: 'Microstructure and nanohardness of cold-sprayed depositionss: electron backscattered diffraction and nanoindentation studies', *Scr. Mater.*, 2010, **62**, 395–398.
6. P. C. King, A. J. Poole, S. Horne, R. de Nys, S. Gulizia and M. Z. Jahedi: 'Embedment of copper particles into polymers by cold spray', *Surf. Coat. Technol.*, 2013, **216**, 60–67.
7. N. Cincaa, J. M. Rebledb, S. Estradé, F. Peiró, J. Fernández and J. M. Guilemanya: 'Influence of the particle morphology on the Cold Gas Spray deposition behavior of titanium on aluminum light alloys', *J. Alloys Compd*, 2013, **554**, 89–96.
8. T. Goyal, R. S. Walia and T. S. Sidhu: 'Surface roughness optimization of cold-sprayed depositionss using Taguchi method', *Int. J. Adv. Manuf. Technol.*, 2012, **60**, 611–623.
9. C. K.S. Moy, J. Cairney, G. Ranzi, M. Jahedi and S. P. Ringer: 'Investigating the microstructure and composition of cold gas-dynamic spray (CGDS) Ti powder deposited on Al 6063 substrate', *Surf. Coat. Technol.*, 2010, **204**, 3739–3749.
10. L. Ajdelsztajn, B. Jodoin, G. E. Kim and J. M. Schoenung: 'Cold spray deposition of nanocrystalline aluminum alloys', *Metall. Mater. Trans. A*, 2005, **36A**, 657.
11. L. Ajdelsztajn, A. Zúñiga, B. Jodoin, and E. J. Lavernia: 'Cold gas dynamic spraying of a high temperature Al alloy', *Surf. Coat. Technol.*, 2006, **201**, 2109–2116.
12. K. Balani, A. Agarwal, S. Seal and J. Karthikeyan: 'Transmission electron microscopy of cold sprayed 1100 aluminum depositions', *Scr. Mater.*, 2005, **53**, 845–850.
13. P. Lejcek: 'Grain boundary segregation in metals'; 2010, New York, Springer-Verlag.
14. A. A. Nazarov, A. E. Romanov and R. Z. Valiev: 'On the structure, stress fields and energy of non-equilibrium grain boundaries', *Acta Metall.*, 1993, **41**, 1033–1040.
15. R. Kirchheim: 'Reducing grain boundary, dislocation line and vacancy formation energies by solute segregation. I. Theoretical background', *Acta Mater.*, 2007, **55**, 5129.
16. R. Kirchheim: 'Reducing grain boundary, dislocation line and vacancy formation energies by solute segregation: II. Experimental evidence and consequences', *Acta Mater.*, 2007, **55**, 5139.
17. L.S. Shvindlerman, E. Jannot and G. Gottstein: 'On precipitation-controlled grain size in the presence of solute segregation', *Acta Mater.*, 2007, **55**, 3397–3401.
18. T. W. Heo, S. Bhattacharyya and L. Q. Chen: 'A phase field study of strain energy effects on solute-grain boundary interactions', *Acta Mater.*, 2011, **59**, 7800–7815.
19. J. Schäfer, A. Stukowski and K. Albe: 'Plastic deformation of nanocrystalline Pd–Au alloys: on the interplay of grain boundary solute segregation, fault energies and grain size', *Acta Mater.*, 2011, **59**, 2957–2968.
20. X. Sauvage and Y. Ivanisenko: 'The role of carbon segregation on nanocrystallisation of pearlitic steels processed by severe plastic deformation', *Mater. Sci.*, 2007, **42**, 1615.
21. X. Sauvagea, G. Wildeb, S. V. Divinskib, Z. Horitac and R. Z. Valievd: 'Grain boundaries in ultrafine grained materials processed by severe plastic deformation and related phenomena', *Mater. Sci. Eng. A*, 2012, **A540**, 1–12.
22. M. R. Rokni, A. Zarei-Hanzakia, A. A. Roostaei and H. R. Abedi: 'An investigation into the hot deformation characteristics of 7075 aluminum alloy', *Mater. Des.*, 2011, **32**, 2339–2344.
23. K. Hockauf, L. W. Meyer, M. Hockauf and T. Halle: 'Improvement of strength and ductility for a 6056 aluminum alloy achieved by a combination of equal-channel angular pressing and aging treatment', *Mater. Sci.*, 2010, **45**, 4754–60.
24. F. J. Humphreys and M. Hatherly: 'Recrystallization and related annealing phenomena', 2nd edn; 2004, Amsterdam, Elsevier.
25. X. L. Wang, C. T. Liu, U. Keiderling, A. D. Stoica, L. Yang, M. K. Miller, C. L. Fu, D. Ma and K. An: 'Unusual thermal stability of nano-structured ferritic alloys', *J. Alloys Compd*, 2012, **529**, 96–101.
26. G. Sha, L. Yao, X. Z. Liao, S. P. Ringer, Z. C. Duan and G. Terence: 'Langdon segregation of solute elements at grain boundaries in an ultrafine grained Al–Zn–Mg–Cu alloy', *Ultramicroscopy*, 2011, **111**, 500–505.
27. N. Ma, S. A. Dregia and Y. Wang: 'Solute segregation transition and drag force on grain boundaries', *Acta Mater.*, 2003, **51**, 3687–3700.
28. Y. Y. Zhang, X. K. Wu, H. Cui and J. S. Zhang: 'Cold-spray processing of a high density nanocrystalline aluminum alloy 2009 depositions using a mixture of as-atomized and as-cryomilled powders', *Therm. Spray Technol.*, 2011, **20**, 1125–1132.
29. J. D. Embury and R. B. Nicholson: 'The nucleation of precipitates: the system Al–Zn–Mg', *Acta Metall.*, 1963, **11**, 347.
30. M. R. Rokni, A. Zarei-Hanzakia and H. R. Abedi: 'Microstructure evolution and mechanical properties of back extruded 7075 aluminum alloy at elevated temperatures', *Mater. Sci. Eng. A*, 2012, **A532**, 593–600.
31. A. Etienne, B. Radiguet, N. J. Cunningham, G. R. Odette and P. Pareige: 'Atomic scale investigation of radiation-induced segregation in austenitic stainless steels', *Nucl. Mater.*, 2010, **406**, 244.
32. G. Sha, R. K. W. Marcea, X. Gao, B. C. Muddle and S. P. Ringe: 'Nanostructure of aluminium alloy 2024: segregation, clustering and precipitation processes', *Acta Mater.*, 2011, **59**, 1659–1670.
33. C. Panseri, F. Gatto and T. Federighi: 'Interaction between solute magnesium atoms and vacancies in aluminium', *Acta Metall.*, 1958, **6**, 198.
34. G. P. Purja Pun and Y. Mishin: 'A molecular dynamics study of self-diffusion in the cores of screw and edge dislocations in aluminum', *Acta Mater.*, 2009, **57**, 5531–5542.
35. R. C. Picu and D. Zhang: 'Atomistic study of pipe diffusion in Al–Mg alloys', *Acta Mater.*, 2004, **52**, 161.
36. Y. Gao, Z. Zhuang, Z. L. Liu, X. C. You, X. C. Zhao and Z. H. Zhang: 'Investigations of pipe-diffusion-based dislocation climb by discrete dislocation dynamics', *Int. J. Plast.*, 2011, **27**, 1055–1071.
37. T. Fujita, Z. Horita and T. G. Langdon: 'Characteristics of diffusion in Al–Mg alloys with ultrafine grain sizes', *Philos. Mag. A*, 2002, **82A**, 2249.
38. J. D. Rittner and D. N. Seidman: 'Solute-atom segregation to <110> symmetric tilt grain boundaries', *Acta Mater.*, 1997, **45**, 3191–3202.
39. A. Varschavsky and E. Donoso: 'A calorimetric investigation on the kinetics of solute segregation to partial dislocations in Cu–3·34at%Sn', *Mater. Sci. Eng. A*, 1998, **A251**, 208–215.
40. M. A. Puigví, A. Serra, N. de Diego, Yu. N. Osetsky and D. J. Bacon: 'Features of the interactions between a vacancy and interstitial loops in metals', *Philos. Mag. Lett.*, 2004, **84**, 257.
41. F. Gärtner, T. Stoltenhoff, J. Voyer, H. Kreye, S. Riekehr and M. Koçak: 'Mechanical properties of cold-sprayed and thermally

sprayed copper depositionss', *Surf. Coat. Technol.*, 2006, **200**, 6770–6782.
42. T. S. Hudson, S. L. Dudarev and A. P. Sutton: 'Confinement of interstitial cluster diffusion by oversized solute atoms', *Proc. R. Soc. Lond. A*, 2004, **460A**, 2457.
43. K. T. Aust and J. W. Rutter: *Trans. AIME*, 1959, **215**, 119–127.
44. G. A. Edwards, K. Stiller, G. L. Dunlop and M. J. Couper: 'The precipitation sequence in Al–Mg–Si alloys', *Acta Mater.*, 1998, **46**, 3893–3904.